

An HST/NICMOS view of the prototypical giant H II region NGC 604 in M33

Rodolfo H. Barbá¹ • Jesús Maíz Apellániz² •
Enrique Pérez • Mónica Rubio • Alberto Bolatto³
• Cecilia Fariña⁴ • Guillermo Bosch^{1,4} •
Nolan R. Walborn

© Springer-Verlag ●●●

Abstract We present the first high-spatial resolution near-infrared (NIR) imaging of NGC 604, obtained with the NICMOS camera aboard the Hubble Space Telescope (HST). These NICMOS broadband images reveal new NIR point sources, clusters, and diffuse structures. We found an excellent spatial correlation between the 8.4 GHz radio continuum and the 2.2 μm nebular emission. Moreover, massive young stellar object candidates appear aligned with these radio peaks, reinforcing the idea that those areas are star-forming regions. Three different scaled OB associations are recognized in the

NICMOS images. The brightest NIR sources in our images have properties that suggest that they are red supergiant stars, of which one of them was previously known. This preliminary analysis of the NICMOS images shows the complexity of the stellar content of the NGC 604 nebula.

Keywords galaxies: starburst – HII Regions – ISM: individual (NGC 604) – Messier 33 – stars: red supergiants – stars: early-type – stars: formation

1 Motivation for a detailed study of NGC 604

Giant H II regions (GHRs) are among the most luminous objects that can be individually identified very distant galaxies. In these regions star formation occurs at extremely high rates, hence they are also known as starburst regions. Given the young age and large number of massive stars in GHRs, some of them are still found embedded in their dusty parental molecular clouds. The morphology of these regions changes quite rapidly during the first few million years after the first massive generation is born. Excellent pictures showing these evolutionary morphologies are the H II regions in the irregular galaxy NGC 4214 (Maíz Apellániz 2000; MacKenty et al. 2000).

The natural extension to larger scales are the starburst galaxies which can be observed at cosmological distances and, therefore, can be used as astrophysical signposts to trace the star formation history of the Universe. However, due to their large distances, we must rely only on their major global properties, such as the behavior of the strong recombination lines originating in the ionized nebula. In order to improve our knowledge of these objects in distant galaxies, it is necessary to study resolved nearby examples. 30 Doradus in the LMC and NGC 604 in M33 are the two largest GHRs in

Rodolfo H. Barbá

Departamento de Física, Universidad de La Serena, Benavente 980, La Serena, Chile

Jesús Maíz Apellániz

Enrique Pérez

Instituto de Astrofísica de Andalucía-CSIC, Camino bajo de Huétor 50, Granada, Spain

Mónica Rubio

Departamento de Astronomía, Universidad de Chile, Santiago, Chile

Alberto Bolatto

Dept. of Astronomy and Laboratory for Millimeter-Wave Astronomy, University of Maryland, College Park, MD 20742, USA

Cecilia Fariña

Guillermo Bosch

Facultad de Ciencias Astronómicas y Geofísicas, Universidad Nacional de La Plata, Argentina

Nolan R. Walborn

Space Telescope Science Institute, 3700 San Martin Dr., Baltimore, MD 21218, USA

¹Member of the Carrera del Investigador Científico CONICET, Argentina

²Ramón y Cajal Fellow

³Department of Astronomy and Radio Astronomy Laboratory, University of California, Berkeley, CA 94720, USA

⁴Instituto de Astrofísica La Plata, CONICET, La Plata, Argentina

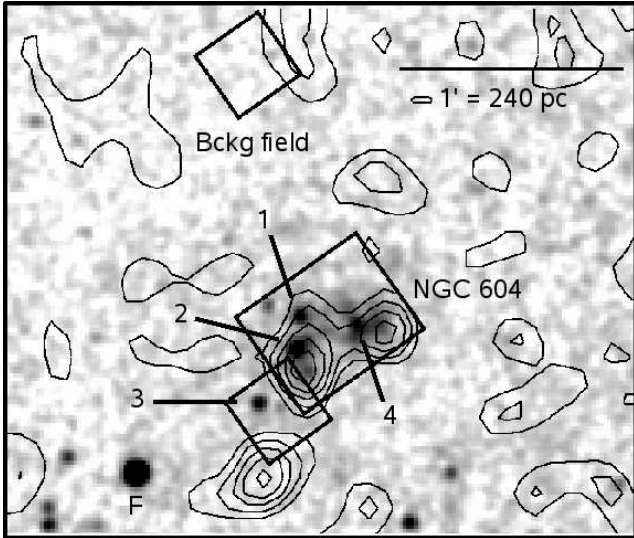


Fig. 1 2MASS K_s -band image of the region of NGC 604. IR sources labeled as 1, 2, 3, and 4 are associated directly with the molecular clouds (contours, adapted from Engargiola et al. 2003). Fields observed with the NICMOS camera 2 are marked as rectangles in full lines. North is up and East to the left. The point source labeled as “F” is a galactic foreground star.

the Local Group (LG), so they are the prime candidates for such study.

NGC 604 is located at a distance of 840 kpc (Freedman et al. 2001). At such a distance, $1''$ is equivalent to 4 pc and consequently the capabilities of HST are essential to study the region with high spatial resolution. NGC 604 is powered by a massive young cluster without a central core that contains over 200 O and WR stars (Maíz Apellániz 2001 and references therein). This GHR is the best nearby example of a scaled OB association, or SOBA, as defined by Maíz Apellániz (2001), a more extended type of object than 30 Dor, which is a Super Star Cluster (SSC). The combination of similarities and differences between those objects makes the combined analysis of both 30 Doradus and NGC 604 a necessary step for the creation of a template for the understanding of far-away starbursts.

In this contribution we describe the gathered observations and general objectives, and we present a preliminary analysis of the new HST/NICMOS images.

2 Observations

We are dedicating a large observational effort to do a thorough multi-wavelength study of NGC 604, from the far ultraviolet to the near infrared with additional high-resolution millimetric observations, combining existing data with the new ones. The new HST data are divided

into three sets: (a) slitless objective-prism FUV spectroscopy obtained using ACS/SBC, (b) multi-filter (6 broadband and 2 narrowband) NUV to optical imaging obtained using ACS/HRC, and (c) NICMOS/NIC2 broadband imaging. These datasets were obtained under HST proposals 10419 and 10722. The existing data include STIS-NUV objective-prism spectroscopy and photometry obtained under HST/GO program 9096, as well as archival HST/WFPC2 imaging. Additional observations were obtained using Gemini North/NIRI in 3 broadband and 3 narrowband NIR filters and with the Combined Array for Research in Millimeter-wave Astronomy (CARMA) in multi-configurations C, D, and E, to observe the CO($1 \rightarrow 0$) transition with a velocity resolution of 3 km s^{-1} , and a beam size ranging from $3''$ - $5''$.

The main goals of this project are: to obtain spectral classifications for about 200 stars, measuring their spectral energy distribution (SED) from 130 nm to $2.2 \mu\text{m}$, to identify embedded very young stellar populations hidden inside dust clouds, to measure the extinction law and its possible variations as a function of the environmental conditions, and to analyze the relationship between the hot stars and the surrounding gas. The combination of all data will allow to obtain the most complete and detailed extinction corrected Hertzsprung-Russell diagram of a resolved SOBA. The SEDs obtained will be analyzed with CHORIZOS (Maíz Apellániz 2004) as the primary code.

3 A NICMOS view of NGC 604

Six *HST* orbits were requested and allocated to observe six selected fields in and near NGC 604 with the NICMOS camera 2 (NIC2), using the broadband filters F110W, F160W and F205W (similar to the J , H , and K passbands, respectively). Figure 1 shows the observed fields on a K_s image extracted from 2MASS. A $37'' \times 32''$ (~ 140 pc) area centered on the core of NGC 604 was observed in four tiles using a dithering strategy. An adjacent field to the south of the core, centered on a bright NIR source was also observed. In addition, sky frames were obtained in a nearby ($1' \equiv 240$ pc away) field for background subtraction and to take into account the stellar population of the M33 disk in the subsequent photometric analysis.

Molecular clouds associated with NGC 604 have been detected in CO by Engargiola et al. (2003 and references therein). The 2MASS K_s -band image (Fig. 1) shows a concentration of point-like sources in the core of NGC 604, some of them surrounded by an extended

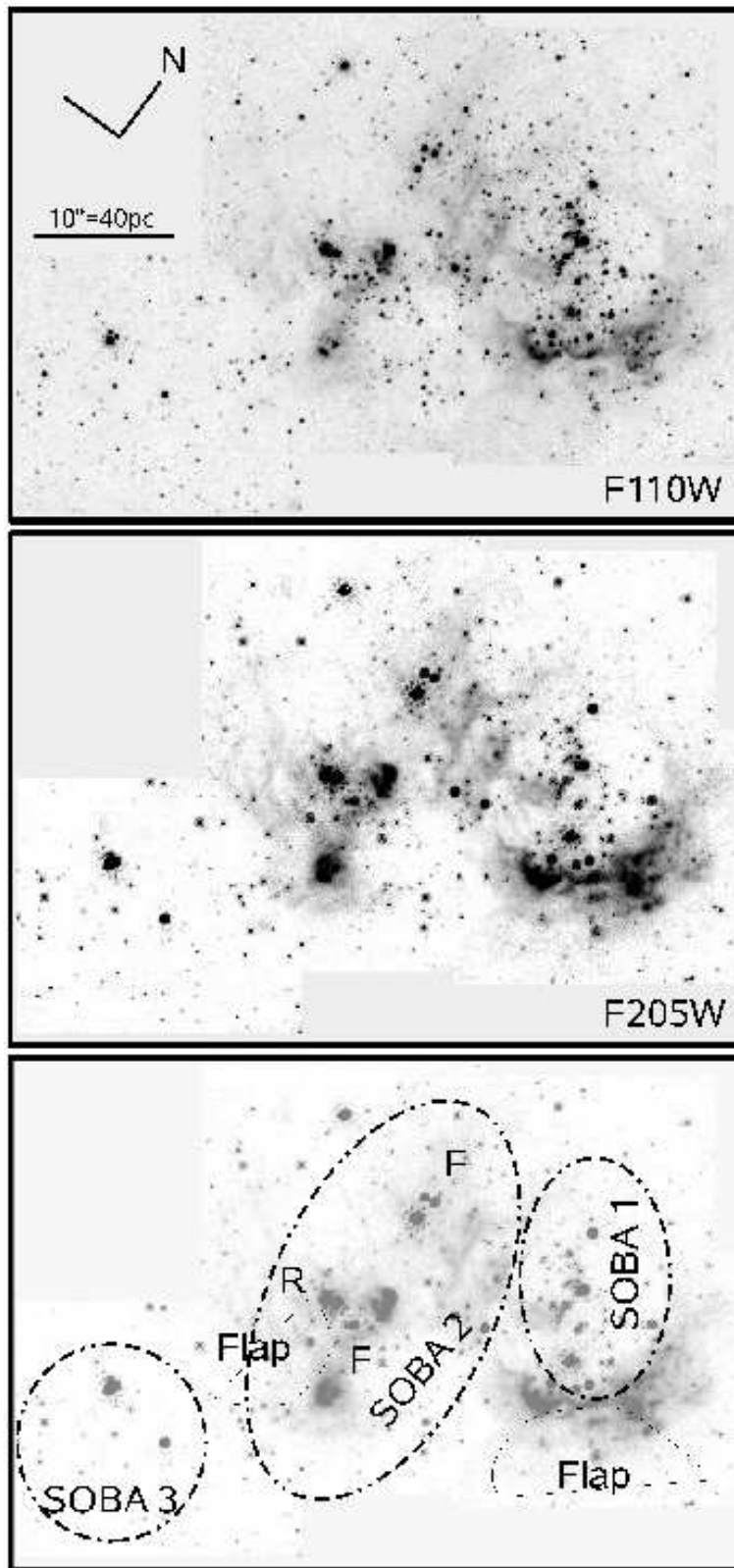


Fig. 2 NICMOS F110W (top panel) and F205W (middle panel) mosaics of NGC 604. The bottom panel is an explanatory diagram for some structures discussed in the text. SOBAs labeled as “1”, “2” and “3” are the main SOBA, the secondary SOBA and a third one located to the south, respectively. The “F” letter indicates the optically visible gaseous filaments. Flaps are areas with high optical extinction. “R” refers to the red supergiant star discovered by Terlevich et al. (1996)

halo. In contrast, the “background” field seems clean of such bright sources. The 2MASS IR sources are associated directly with the molecular clouds. This morphological relationship between infrared sources and molecular clouds resembles the 30 Dor Nebula.

The new NICMOS broadband imaging of NGC 604 reveals new IR point sources, clusters and diffuse structures, improving the spatial resolution of the 2MASS data by more than an order of magnitude. Figure 2 shows the F110W and F205W mosaics of five NIC2 fields in the observed area of NGC 604. The variety of observed structures is striking. The two optically detected SOBAs (main and secondary) are easy to discern. They are encircled by labeled ellipses in Fig. 2 (see Maíz Apellániz et al. 2004 for detailed explanation of the optical structures). An additional SOBA affected by larger extinction is present to the south (labeled as “SOBA 3”). The two cavities associated to the SOBAs are defined. Cavity A (associated to the main SOBA) is limited by a bright rim to the south. This rim is brighter in the F205W filter, when compared with the F110W filter, indicating that it is affected by a large extinction. The extended nebular emission to the southwest in the F205W image is coincident with the structure labeled as “flap” by Maíz Apellániz et al. (2004), an (optical) obscuration area which is a dusty screen associated with the molecular cloud in that region. This main CO cloud lies on the southern edge of the bright nebular rim. Churchwell & Goss (1999) and Maíz Apellániz et al. (2004) have analyzed the extinction in NGC 604 using radio continuum, $H\alpha$, and $H\beta$ images. They have found a very good correlation between the CO emission and the total optical extinction, which indicates that the dust is associated with molecular gas. Some of the H II gas is located behind large-optical-depth well-defined dust “flaps” that make it invisible in the optical. Figure 3 shows the 8.4 GHz radio continuum contours (from (Churchwell & Goss 1999)) superimposed on the F205W image. Again, the correlation between radio and $2.2\mu\text{m}$ emission seems to be very good. The radio peaks C and D are superposed to the southwest NIR nebular emission. The radio peaks A and B are coincident with nebular knots. Peak A is one of the brightest $H\alpha$ structures (see (Maíz Apellániz et al. 2004)), and the same happens in the NIR. Gemini/NIRI images (not shown) demonstrate that most of such emission is produced in the warm gas as Brackett γ emission line. A very interesting result is the remarkable spatial correlation between the massive young stellar object candidates and the radio peaks, which suggests that those areas are prime candidates for massive star forming regions.

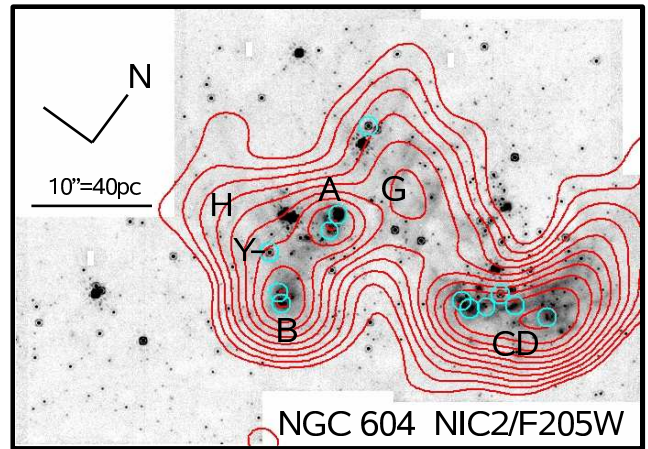


Fig. 3 Contour diagram of the 8.4 GHz radio continuum (adapted from Churchwell & Goss 1999) superposed on the F205W NIC2 image. Labels indicate the radio continuum structures (see Maíz Apellániz et al. 2004 for an explanation). Circles mark the position of the massive young stellar object candidates

4 NICMOS photometry

Point spread function photometry was performed in the NIC2 mosaics and “background” field. In total, we have more than 600 detections in the three filters with photometric errors less than 0.3 mag. The photometric sensitivity is about 21.9 mag in the F205W filter, corresponding to an unreddened early-B type star at the distance of M33. Figure 4 shows the color-color and color-magnitude diagrams for all sources brighter than $m_{F205W} = 19.5$ (O3 V star at M33). We decided to preserve our data in the NICMOS photometric system in order to avoid additional problems with color transformations to ground-based photometric systems. Main-sequence and red giant stars loci are plotted as continuum lines in the color-color diagram in Fig. 4. They are synthesized using CHORIZOS, Kurucz models, and NIC2 filter transmission curves. Reddening vectors ($A_V = 16$) for an early-type star and a red giant have been derived in the same way, adopting a normal reddening law. In the color-color diagram is possible to discern three main population of objects: (a) *blue, hot* stars with small or moderate reddening close to the main-sequence locus and along the reddening track; (b) *red* stars in the red giant locus; (c) a population of stars with infrared excess to the right of the early-type star reddening vector.

The distribution of sources in the color-magnitude diagram shows that the *blue* sources (group a) correspond mostly to luminous hot stars associated to SOBAs (massive stars). Meanwhile, stars in the group (c) are mostly massive young stellar object (MYSO)

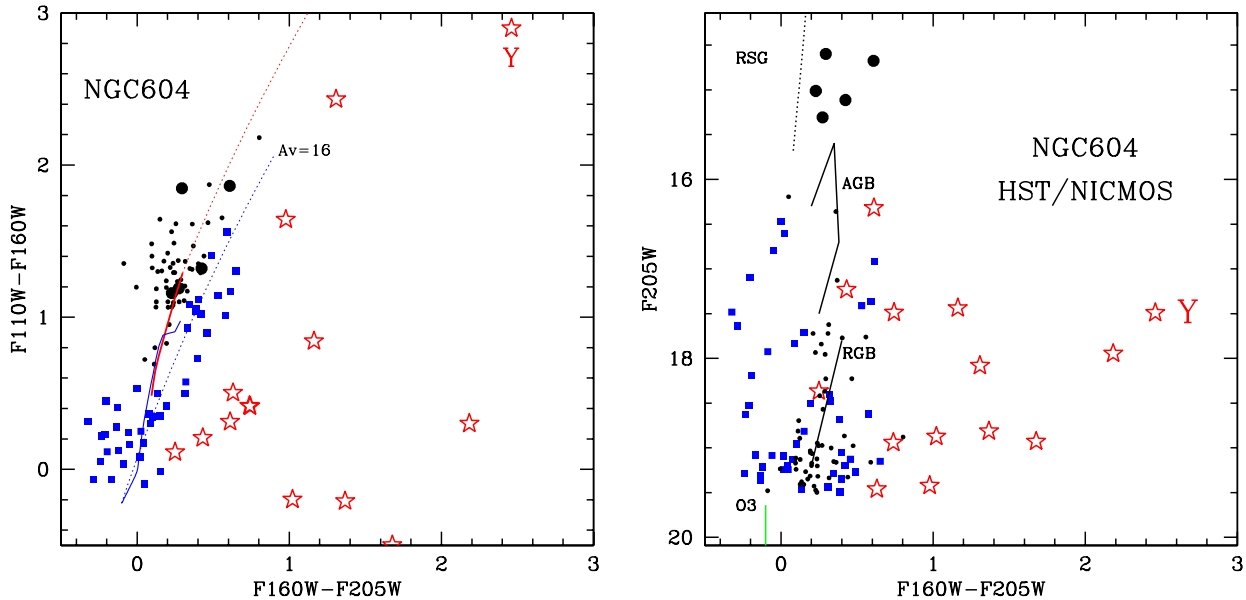


Fig. 4 NIC2 color-color (left) and color-magnitude (right) diagrams. This plot includes all sources with $m_{F205W} < 19.5$. Color-color diagram: the main-sequence locus and the cool-giant branch are indicated as solid lines; reddening tracks for $A_V = 16$ are also plotted. Color-magnitude diagram: red supergiant star locus is indicated as a dotted line in the upper part of the diagram; the asymptotic giant branch and red giant branch are also plotted as full lines. Symbols: “stars” are MYSO candidates; “squares” are hot stars; “dots” are mostly red giant stars; “black circles” are red supergiants stars

candidates and/or extreme emission line objects. Objects in group (b) are stars belonging to the red giant branch, and they are more or less smoothly distributed in the mosaic. The brightest objects in the field are five stars in group (b). Their positions in the color-magnitude diagram suggest that they are red supergiant stars. In fact, one of them has been spectroscopically identified as such by Terlevich et al. (1996). This star is a close companion to a compact massive cluster and two WR star candidates (WR11 and WR7, see Drissen et al. 1993 and Maíz Apellániz et al. 2004). The other four red supergiant star candidates are also located very close (few arc-seconds) to bona-fide WR stars, WR candidates or massive hot stars. The spatial neighborhood observed between the RSG stars and the early-type objects addresses the question of whether they belong to the same star generation or they just represent a superposition of different populations, as it is the case of 30 Dor. In the latter GHR, Walborn & Blades (1997) proposed the coeval existence of five distinct populations, nicely distinguished by age and distribution. Likewise, this issue indicates the complexity of the stellar content in a GHR.

Among the MYSO candidates, a particular source deserves special consideration, owing to its large NIR colors. This object, labeled as “Y” in Fig fig:radio and Fig. 4 is barely detectable in the F110W image. Its NIR photometric properties are very similar to those of the

MYSO in 30 Dor (Rubio et al. 1998; Brandner et al. 2001), indicating large luminosity. The source Y is located in a region of very large extinction, close ($2''$) to a filled H II region (radio peak B) and the molecular cloud core. Thus, this area has all the necessary ingredients to be a star forming region.

5 Summary

In this contribution we have presented the first high-spatial resolution NIR images of NGC 604, obtained with the NIC2 camera aboard *HST*. These new NICMOS broadband images reveal new NIR point sources, clusters and diffuse structures. We found an excellent spatial correlation between 8.4 GHz radio continuum and $2.2 \mu\text{m}$ nebular emission. We also found that MYSO candidates appear aligned with those radio peak structures, reinforcing the idea that those areas are star-forming regions. Three different SOBAs can be recognized in the new NICMOS images. moreover, the brightest NIR sources in our images show properties that suggest the presence of RSG stars.

This preliminary analysis of the NICMOS images shows the extreme complexity of the stellar content in the NGC 604 nebula.

Acknowledgements RHB would like to thank the Scientific Organizing Committee for the invitation to participate in the meeting and the IAA staff and Director for the warm hospitality during his visit to the Institute. We would like to thank Greg Engargiola and Ed Churchwell for giving us access to their data. Support for this work was provided by FONDECYT Project No. 1050052 (RHB), by the Chilean *Center for Astrophysics* FONDAF No. 10510003 (MR), and by the Spanish Ministerio de Educación y Ciencia (JMA and EP) through the Ramón y Cajal program and grants AYA2004-02703 and AYA2007-64712, which are co-financed with FEDER funds.

References

- Brandner, W., Grebel, E. K., Barbá, R. H., Walborn, N. R., & Moneti, A. 2001, *Astron. J.*, 122, 858
- Churchwell, E., & Goss, M. 1999, *Astrophys. J.*, 514, 188
- Drissen, L., Moffat, A. F. J., Shara, M. M. 1993, *Astron. J.*, 105, 1400
- Engargiola, G., Plambeck, R. L., Rosolowsky, E., & Blitz, L. 2003, *Astrophys. J. Suppl. Ser.*, 149, 343
- Freedman, W. L., et al. 2001, *Astrophys. J.*, 553, 47
- MacKenty, J., Maíz Apellániz, J., Pickens, C., Norman, C., & Walborn, N. R. 2000, *Astron. J.*, 120, 3007
- Maíz Apellániz, J. 2000, *Publ. Astron. Soc. Pac.*, 112, 1138
- Maíz Apellániz, J. 2001, *Astrophys. J.*, 563, 151
- Maíz Apellániz, J. 2004, *Publ. Astron. Soc. Pac.*, 116, 859
- Maíz Apellániz, J., Pérez, E., & Mas-Hesse, J. M. 2004, *Astron. J.*, 128, 1196
- Rubio, M., Barbá, R. H., Walborn, N. R., Probst, R. G., García, J., & Roth, M. R. 1998, *Astron. J.*, 116, 1708
- Terlevich, E., Díaz, A. I., Terlevich, R., González Delgado, R. M., Pérez, E., & García-Vargas, M. L. 1996, *MNRAS*, 279, 1219
- Walborn, N. R., & Blades, C. 1997, *Astrophys. J. Suppl. Ser.*, 112, 457